Exploring the interaction between polystyrene nanoplastics and *Allium cepa* during germination: internalization in root cells, induction of toxicity and oxidative stress

Lucia Giorgetti [1 *°], Carmelina Spanò [2-3°], Simonetta Muccifora [4], Stefania Bottega [2], Francesco Barbieri [4], Lorenza Bellani [1-4], Monica Ruffini Castiglione [2-3]

[1] Institute of Agricultural Biology and Biotechnology, (IBBA-CNR), Pisa; [2] Department of Biology, University of Pisa; [3] Centre for Climate Change Impact, University of Pisa; [4] Department of Life Sciences, University of Siena

° co-first authors

*Corresponding author: Lucia Giorgetti, Institute of Agricultural Biology and Biotechnology, National Research Council (IBBA-CNR), via G. Moruzzi, 1 - 56124 Pisa, Italy. E-mail: lucia.giorgetti@ibba.cnr.it

ABSTRACT

With the aim to investigate the mechanisms of action of nano plastics (nano PS) on plants, seeds of *Allium cepa* were germinated for 72 h in the presence of polystyrene nano PS (50 nm size, at concentrations of 0.01, 0.1 and 1 g L^{-1}) and, subsequently, roots were analysed by a multifaceted approach. No effect was induced by any concentration of nano PS on the percentage of seed germination while root growth was inhibited by 0.1 and 1 g L^{-1} nano PS. Cytological analysis of the root meristems indicated cytotoxicity (reduction of mitotic index) and genotoxicity (induction of cytogenetic anomalies and micronuclei) starting from the lowest dose. Moreover, the biochemical and histochemical analysis of oxidative stress markers gave evidence of stress induction, especially at the highest doses. Damages reported could be due to mechanical surface contact in root external layers, as evidenced by histological localization, and to the internalization of nano PS in different cellular compartments, observed under TEM. The present research underlines the hazardous nature of nano PS, that for their ability to be internalized into crop plants, can enter into different trophic levels of the food chain.

Key words: *Allium cepa* L., genotoxicity, oxidative stress, polystyrene nanoplastics, ultrastructural analysis.

- **Cyto-physiological traits in onion roots treated by nano-polystyrene were studied**
- **Nano PS reduced root elongation in onion seedlings during germination**
- **Nano PS induced cyto/genotoxicity on root meristem**
- **The highest applied concentrations of nano PS triggered oxidative stress**
- **Nano PS were internalized in different root cellular compartments**

1. INTRODUCTION

The production of plastics and their use in many industrial sectors as low-cost, innovative and resistant materials is relatively recent as it began around the 1950s. Since then, plastics adoption for new technologies and everyday life have grown exponentially. Plastics are employed for packaging, building and construction, electrical and electronics, agriculture, medical and pharmaceutical applications, household and many other sectors (Geyer et al., 2017). It is estimated that in 2017 the worldwide production of plastics was 348 million tons, about 64 million tons of which in Europe (Plastics Europe, 2018). Unfortunately, such a high use of plastics and the poor attention to their discharge and recycling are causing the production of huge amount of waste which may give rise to global contamination in all environmental matrices. The classification of plastics in aquatic and terrestrial matrices evidenced that synthetic polymers like polyethylene, polyvinyl chloride, polypropylene, polyethylene terephthalate, polyamide (nylon), polyester and polystyrene are the most frequently detected in all the environments (Rochman et al., 2013; Duis and Coors, 2016). As these plastics are not biodegradable, they remain in the environment for a very long time undergoing aging processing for chemical and physical environmental activities, resulting in plastic fragmentation into smaller pieces, from larger plastics debris up to micro (less than 5 mm) and nano (less than 100 nm) particles dimension (Barnes et al., 2009; Mattsson et al., 2015). In light of this, particular attention is addressed to plastic dimensions, to the polymer basic structure and to the capacity to adsorb toxic organic and inorganic pollutants like persistent organic pollutants and metals (Hidalgo-Ruz et al., 2012). These variables can be crucial in determining the level of toxicity of plastics in exposed organisms.

Discharged plastic material flows from land to freshwater, waterways and seas, giving rise to pollution of aquatic ecosystems.

Besides, soil contamination by plastics can occur from domestic sewage (containing synthetic fibres from clothes and microbeads from cosmetics and personal care products), from biosolid, from

irrigation with wastewaters, from plastic mulch used in agriculture, landfill and from uncontrolled discharge into the environment (Chae and An, 2018; Ng et al., 2018).

At present, most of ecotoxicological studies focuses on aquatic and marine environments and the impact of plastics, on populations at various trophic levels, also considering the possible transmission from aquatic to terrestrial organisms (Hammer et al., 2012). These studies basically report the effects of microplastics on marine organisms' growth, life cycle, reproduction and mortality, and neurotoxic, genotoxic, cytotoxic effects, oxidative stress and alteration of blood and haemolymph parameters (de Sá et al., 2018).

The terrestrial environment has so far been less studied than the marine one (de Souza Machado et al., 2018), probably for the complexity of the soil matrix, in respect to water. Plastic particles, as debris, micro- and nano PS, can be incorporated into the soil structure, while in water they remain in suspension or settle on the seabed. The direct absorption or ingestion of micro and nano PS by marine organisms at different trophic levels, is universally ascertained and documented (Alimba and Faggio, 2019) since it can be detected more likely than incorporation of plastics by terrestrial organisms. Recent studies demonstrated that microplastic can directly enter the food chain through soil micro and macrofauna (Huerta Lwanga et al., 2017; Zhu et al., 2018).

Agriculture ecosystems appear to be the most polluted by plastics for the commonly adopted cultivation practices. Despite the possible internalization of these potentially toxic compounds in plant tissues and the transfer to animals and humans through the food chain, information on the effects of micro and nano PS on plants is currently very scarce. Up to now few studies have investigated the effects of micro- nano PS on non-vascular plants (Sjollema et al., 2016; Nolte et al., 2017; Prata et al., 2019), and studies on tracheophytes are just beginning to be available in the scientific literature. Most of these publications is focused on the effects of micro- nano PS on plant growth and biomass production (Kalčíková et al., 2017; Qi et al., 2018; Boots et al., 2019; Bosker et al., 2019; van Weert et al., 2019). Deeper investigations on nano PS and crop species have been

published by Jiang et al. (2019) and Lian et al. (2020) on *Vicia faba* and *Triticum aestivum* respectively.

In light of this the present work was planned to explore plant-nano PS interactions with a multidisciplinary approach. *Allium cepa* has been chosen as a model plant for phyto and genotoxicity tests, with the aim to clarify the mechanicistic processes behind plant response following treatments with nano PS (50 nm size). An environmentally relevant concentration <15 μg L^{-1} for nano PS has been proposed for studies reproducing plastic pollution in marine ecosystems (Al-Sid-Cheikh et al., 2018). Even if realistic concentrations of nano PS in soils are not easy to predict with modelling systems, nano PS may occur in soil at higher levels than in marine ecosystems, by at least a factor of four (Hayes, 2019). Based on these indications, concentrations of 0.01, 0.1 and 1 g L^{-1} nano PS have been used.

The different endpoints evaluated the effects of nano PS on seeds germination, on root length, on mitotic activities, on the presence of cytogenetic abnormalities and micronuclei in root meristem. Moreover, oxidative stress markers and TEM analysis of root structure allowed to further assess the toxic effects of nano PS, their possible internalization and ultrastructural modifications in plant cells.

2. MATERIALS AND METHODS

2.1. Polystyrene nanoparticles and plant material

Red Polystyrene microspheres, Visiblex TM Color Dyed Microspheres, nominal size 50 nm, were purchased by Phosphorex, Inc. (South St. Hopkinton, MA01748).

Seeds of *Allium cepa* L. var. Tropea rossa tonda (organic certified IT BIO 009) were germinated in the dark at 24 ±1 °C in small wells with 200 μl of distilled water (control, C) or with a suspension of red polystyrene microspheres (nano PS) at the concentrations of 0.01, 0.1 and 1 g L^{-1} for 72 hours in two separate experiments. After 72h of germination seedlings were carefully and

vigorously washed in deionized water and roots were collected and used fresh or fixed as indicated below.

2.2. Phytotoxicity, cytotoxicity and genotoxiciy tests

Phytotoxicity test was performed scoring both seed germination rate (% germinated seeds) and root length in four replicates of 10 seeds for each sample (ISO 11269-I).

Ten roots for each treatment were fixed in ethanol/glacial acetic acid (3:1 v/v). Root tips were squashed and stained following Feulgen technique as described in Giorgetti and Ruffini Castiglione (2016). At least 1000 nuclei were analysed randomly for each slide with five replicates for each treatment by light microscope, for mitotic activity estimation and for scoring mitotic aberrations and micronuclei frequency.

Mitotic activity was expressed as mitotic index (MI, number of mitosis per 100 nuclei) to indicate the levels of cytotoxicity of the treatments.

Micronucleus frequency assay (MNC test, number of micronuclei per 1000 nuclei) and mitotic aberrations (aberration index AI=number of aberrations per 100 nuclei) were determined for the evaluation of genotoxicity of the treatments.

The aberrations scored included chromosomal bridges and fragments, lagging chromosomes, aberrant metaphases and disturbed anaphases in dividing cells and micronuclei in interphase cells.

2.3. Determination of hydrogen peroxide and thiobarbituric acid reactive substances (TBARS).

Hydrogen peroxide content of roots, stored at -80 °C, was determined according to Jana and Choudhuri (1982). After grounding and homogenization with phosphate buffer 50 mM pH 6, the homogenate was centrifuged at 6000g for 25 min. To determine the H_2O_2 content, extract was mixed with 0.1% titanium chloride in 20% (v/v) H_2SO_4, the mixture was centrifuged at 6000g for 15 min and the absorbance of supernatant was read at 410 nm. The amount of H_2O_2 was calculated from a standard curve and expressed as μmol g^{-1}FW.

Lipid peroxidation in roots, was estimated in terms of TBARS according to Wang et al. (2013) with minor modifications as in Spanò et al. (2017). The concentration of TBARS was expressed as nmol g^{-1} FW, measuring the specific absorbance at 532 nm by subtracting the non-specific absorbance at 600 nm. Calculation were made using an extinction coefficient of 155 mM^{-1} cm^{-1}.

2.4. Histological analysis and in situ oxidative stress

Ten roots of comparable size and length, belonging to plantlets randomly selected for each treatment, were isolated and sectioned with hand microtome, 3-4 mm from the root tip, to explore possible distribution of nano PS aggregates in root tissues with light microscope (Leitz Diaplan Wetzlar, Germany, equipped with a Leica DFC 420 camera, Leica Microsystems, Germany).

Amplex UltraRed Reagent (Life Technologies, USA) was applied to cross sections for *in situ* detection of H_2O_2 (Ruffini Castiglione et al., 2016). After staining, slices were mounted in glycerol and observed with fluorescence microscope (568ex/681em nm). BODIPY 581/591 C11 was applied as a fluorescent marker to visualize lipid peroxidation levels with a change of the fluorescence emission peak from red to green (Ruffini Castiglione et al., 2016). Microscope analysis was performed acquiring simultaneously the green (485ex/510em nm) and the red fluorescence (581ex/591em nm) signals and merging the two images (Kovácik et al., 2014). Fluorescence microscope analysis was carried out with a Leica DMLB, equipped with appropriate set of excitation/emission filters and with a Leica DC300 ccd camera.

2.5. Transmission electron microscope (TEM)

To evaluate the real size of the polystyrene microspheres object of the present study, a drop (10 µl) of the nano PS solution 1 g L^{-1} was placed on TEM grids covered with formvar, allowed to settle and to dry. To analyse particles dimensions, TEM images were analysed with ImageJ programme by measuring the major and the minor axes.

For TEM root observations, the treatments with nano PS 0.1 and 1 g L^{-1} concentration were chosen. Small cubes of control and treated roots were pre-fixed in Karnovsky solution (Karnovsky, 1965), post-fixed in osmium tetroxide, dehydrated and embedded in Epon 812-Araldite A/M mixture. Thin sections were stained with uranyl acetate and lead citrate. Isolated NPs and root sections were observed under a FEI Tecnai G2 Spirit electron microscope at 100 kV.

2.6. Statistical Analysis

All data were reported as mean of replicates ± Standard Deviation (SD). Analysis of variance (ANOVA) and a *post hoc* Tukey HSD multiple range test were used to identify statistically significant differences between treatments using the Statistica package (StatSoft) 6.0 version. Different letters indicate significant differences at $p \leq 0.05$.

3. RESULTS AND DISCUSSION

3.1. TEM nano PS characterization

Nano PS dimensions were determined by analysis of TEM photograph (Figure 1a). As particles generally presented irregular shapes both major and minor axes were measured. Nano PS size ranged from 20 - 190 nm. The average dimensions were 82.93 nm for the major axis and 70.39 nm for the minor axis. Nano PS size was grouped in frequency classes for size distribution (Figure 1b, c) evidencing that 77% of the particles had both axes minor than 100 nm (Figure 1b), while 85% had at least one axis minor than 100 nm (Figure 1c). The most represented frequency class (16%) had minor axis 41 - 50 nm, while particles with both dimensions greater than 100 nm were only 15%. According to the definition currently in use that NPs have at least one dimension inferior than 100 nm, the analyzed sample contained as much as 85% nano PS.

3.2. Seed germination and seedling growth

Germination percentage and root length of *A. cepa* analysed following 72 h nano PS exposure are reported in Table 1 and Figure 2, respectively. Not statistically significant differences were observed in germination percentage among different treatments. On the contrary, root length decreased in a dose dependent manner in all treatments, at 1 g L^{-1} being reduced about 41.5% in respect to the control (Figure 2).

The lack of influence of nano PS on germination process at 72 hours of imbibition is in accordance with Bosker et al. (2019) reporting that the reduction of germination in *Lepidium sativum* at 24 hours completely disappeared at the longer period (72 h). Just recently Lian et al. (2020) confirmed no effects on germination in *Triticum aestivum* seeds treated with nano PS.

The dose-dependent reduction in root elongation is in agreement with growth reduction in roots of *Lemna minor* and *Lepidium sativum* (Kalčíková et al., 2017; Bosker et al., 2019). As hypothesized by Kalčíková et al. (2017), this reduction could be induced by particles adhering to peripheral root tissues. This physical blockage could cause a disturbance in water absorption necessary for the normal imbibition, germination and primary root growth (Bosker et al., 2019). In our system the decrease of root length might also derive from a lower proliferation of root meristem, as demonstrated by the observed reduction of mitotic index.

3.3. Cytotoxicity and genotoxiciy in root meristem

Cytotoxic and genotoxic effects of the different treatments with nano PS were evaluated considering the following endpoints: mitotic index (MI), % of mitotic phases, % of abnormal mitoses and presence of micronuclei (Figure 3).

Inhibitory effect on mitotic activity was observed at 0.1 and 1 g L^{-1} nano PS concentrations while at the lowest concentration (0.01 g L^{-1}) MI was not affected. MI decreased from 9.3% in control meristems to 6.1% and 5.4% in 0.1 and 1 g L^{-1} treatments, corresponding to a decrease of 34.4% and 41.9% respectively (Figure 3a).

The analysis of mitotic phases frequencies, shown in Table 2, indicated that the total percentage of the different mitotic phases was not influenced by nano PS treatments, since a decrease in normal mitotic figures was parallel with an increase of aberrations.

Not statistically significant differences were observed in percentage of normal prophases, metaphases and ana/telophases between control and treatments, but the frequency of abnormal metaphases and ana/telophases increased significantly starting from the lowest dose of nano PS (abnormal metaphases and abnormal ana/telophases being 18.5% and 12.7%, respectively). Interestingly, the highest doses of 0.1 and 1 g L^{-1} did not induce a further increase in cytological anomalies in respect to the lower doses.

Figure 3b highlights the trend in which the total cytological anomalies represent about 30% of the total mitosis, three times higher than the control (10.2%).

The treatments with nano PS induced the formation of several anomalies at different mitotic stages. In particular, it is worth noting that prophases were unaffected by treatments; at metaphase the most common anomalies were c-metaphases, metaphases with lagging and sticky chromosomes (Figure 4a, b, c abnormal c-metaphases, Figure 4d, e sticky metaphases); at ana/telophase sticky chromosomes, lagging and bridges were mainly observed (Figure 4 g-m).

Micronuclei (Figure 3c and Figure 4m, n) were observed in all the nano PS treatments, but differences with the control were significant only at the highest concentration.

Cytological anomalies could be the result of spindle malfunctioning or failure, generating c-metaphase and lagging chromosomes, the latter also associated to a possible delay in the division of centromere. As a consequence, polyploidy or aneuploidy could result in daughter cells. In addition, nano PS treatments exerted a clastogenic effects, as evidenced by the breakage, stickiness or reunion of chromosome observed in root meristems (Figure 4).

Genotoxic effects, associated to oxidative stress, have been recently reported as a consequence of treatments with micro and nano PS in *Vicia faba* (Jiang et al., 2019), in agreement with the effects recorded for metallic nanoparticles (Ruffini Castiglione et al., 2016). Gopinath et al. (2019)

observed higher genotoxic and cytotoxic effects in human blood cells and chromosome aberrations on *A. cepa* roots treated for three hours with nano PS from cosmetics and virgin nano PS (100 nm size, 10 and 25 mg L^{-1}). Also in this case oxidative stress induction or damage to the antioxidative system were proposed as main causes of the recorded cyto/genotoxicity.

3.4. Root histochemical analysis and oxidative stress markers

Figure 5a-d shows representative cross sections of the primary root emerging from the seed following 72 hours of imbibition. The root appeared both diarch and triarch with uniseriate pericycle, endodermis layer with a Casparian strip not always well detectable, thin-walled parenchymatous cells and root epidermis. Nano PS treated roots displayed red areas and/or spots both in the cortical (Figure 5c-d) as well as in the central cylinder (Figure 5b). The red staining in the tegumental tissue (Figure 5d) may be allied to a partial physical/chemical dealing of nano PS with the root surface and could cause a general disturbance in root growth and functioning, as reported for *Lemna minor* (Kalčíková et al., 2017). In addition, our results demonstrated the presence of PS aggregates in different root compartments, suggesting that also nano PS, as other classes of nanoparticles (Geisler-Lee et al., 2013; Deng et al., 2017; Bonilla-Bird et al., 2018; Giorgetti et al., 2019; Bellani et al., 2020), are able to overcome different biological barriers and enter the cells of the roots. This fact is particularly clear when analysing our results of transmission electronic microscopy (see below).

In situ detection of hydrogen peroxide by the specific fluorescent Amplex UltraRed probe showed a weak and flat red signal in the control samples, more intense in the vascular region (Figure 5e). More defined staining pattern was detectable in the treated samples with a responsiveness (Figure 5f-h) particularly intense under 1 g L^{-1} treatment. The latter induced a strong uneven response in the root epidermis and in the cortical cylinder, as well as in the vascular tissues (Figure 5h). BODIPY 581/591 C11 fluorescent probe pointed out an increase in lipid oxidative damages of treated

samples, basically detectable in the tegumental portion as well as in the periphery of the cortical cylinder (Figure 5i-l).

Hydrogen peroxide and TBARS contents, assessed by biochemical analysis (Table 1), significantly increased at the highest nano Ps concentration (Table 1), in line with histochemical results. Noteworthy, under 0.01 g L^{-1} nano Ps treatment the lowest value of TBARS, significantly lower than control, was recorded. Under this treatment, the lowest hydrogen peroxide concentration was also detected, though the difference from control was not significant. The lack of papers focusing on the oxidative stress induced by nano Ps in plants makes it difficult to do a comparative discussion. However, the trend in TBARS content under different concentrations of nano PS is in accordance with the inhibition and induction in MDA by lowest (50 mg L^{-1}) and highest concentrations (100 mg L^{-1}) respectively of 100 nm polystyrene microplastics in *V. faba* roots (Jiang et al., 2019). The induction of oxidative stress by nano PS is also reported in studies on other organisms (Jeong et al., 2018; Sun et al., 2018). Therefore, nanomaterials like metal nanoparticles (Ruffini Castiglione et al., 2016; Giorgetti et al., 2019; Rilling et al., 2019) are able to generate reactive oxygen species (ROS) and consequently oxidative damage. The induction of oxidative stress in terms of H_2O_2 and TBARS increase by nano PS high treatments may be associated with cyto/genotoxicity established with cytological analysis of the root meristem activity. In accordance with Jiang et al. (2019), the antioxidant defence machinery could be sufficient to scavenge ROS at low but not at high concentrations of nanoparticles, when the overproduction of ROS could exceed the antioxidant capacity. However, in this experimental system, cyto/genotoxicity was already established starting from the low PS concentration treatment, at least in terms of mitotic anomalies, suggesting that nano PS might trigger multiple signaling pathways, not only ROS dependent, able to affect cell and genome functioning.

3.5. TEM analysis

Control roots showed cells with large nuclei with 1 or 2 nucleoli, cytoplasms with vacuoles of different sizes, mitochondria, plastids and some electron dense bodies (Figure 6a). The cytoplasm of the nano PS treated cells were often filled with electron dense bodies, probably lipid bodies not yet mobilized, more abundant in 1 g L^{-1} than in 0.1 g L^{-1} nano PS treated roots (Figure 6b). Among these bodies, numerous vacuoles, small mitochondria, dictyosomes and rough endoplasmic reticulum were observed (Figure 6b-d). The internalized nano PS were often observed both in the vacuoles (Figure 6b, c) and in the cytoplasm (Figure 6d, e). They had the cylindrical or parallelepiped shape, sizes from 25 nm to 130 nm and appeared often in the form of aggregates of 2-5 particles (Figure 6c-e). Rarely, nano PS of about 25 nm were detected in nucleus (Figure 6f). The presence of nano PS in the nucleus indicates that probably the smaller nano subfraction of this material may also cross nuclear membrane and interfere with chromatin structure and function. By this way nano PS may contribute to the recorded genotoxic effects, as previously reported for metal nanoparticles in other systems (Shukla et al., 2011; Pakrashi et al., 2014; Bellani et al., 2020). The internalization of nano PS in specific cellular compartments of root tissues by TEM, here reported for the first time, is in accordance with the data of Lian et al. (2020) that showed the presence of nano PS in xylem vessels of wheat by SEM analysis.

The limited mobilization of the lipid reserves observed in the cells of the treated roots was a further relevant data that emerged from the TEM analysis. In parallel, the reported increase in lipid peroxidation, shown by biochemical and histochemical analysis, may involve not only membrane but also reserve lipids (Bailly, 2004), probably causing an impairment in mobilization of lipid reserves (Pedrosa Gomez and Souza Garcia, 2013) and a delay in cell differentiation and root development.

4. CONCLUSIONS

In conclusion, nano PS, in particular at the highest dose, were able to induce cytotoxicy, genotoxicity and oxidative damages in treated roots. On the base of structural and ultrastructural analyses, damages could depend both on mechanical surface contact with the external layers of the root and on the internalization of nano PS in different cellular compartments. Indeed Nano PS might trigger multiple signaling pathways, not only ROS dependent, able to affect cell proliferation/metabolism and genome functioning. Further studies are needed to clarify nano PS intracellular interactions as well as to investigate their effects in long term exposition and their possible translocation from the root to the aerial part of the plant. Considering the ability of food plants to internalize these nanoparticles, with the consequent possible entry into the food chain, the problem of pollution of agricultural land by nano PS is to be urgently considered.

ACKNOWLEDGMENTS

This work was financed by local funding of the University of Pisa (ex 60%) and supported by University of Siena and National Research Council of Italy.

REFERENCES

Alimba, C.G., Faggio, C., 2019. Microplastics in the marine environment: Current trends in environmental pollution and mechanisms of toxicological profile. Environ. Toxicol. Phar. 68, 61-74.

Al-Sid-Cheikh, M., Rowland, S.J., Stevenson, K., Rouleau, C., Henry, T.B., Thompson, R.C., 2018. Uptake, whole-body distribution, and depuration of nanoplastics by the scallop *Pecten maximus* at environmentally realistic concentrations. Environ. Sci. Technol. 52, 14480−14486.

Bailly, C. 2004. Active oxygen species and antioxidants in seed biology. Seed Sci. Res. 14, 93–107.

Barnes, D.K.A., Galgani, F., Thompson, R.C., Barlaz, M., 2009. Accumulation and fragmentation of plastic debris in global environments. Philos. T. Roy. Soc. B. 364, 1985–1998.

Bellani, L., Muccifora, S., Barbieri, F., Tassi, E., Ruffini Castiglione, M., Giorgetti, L., 2020. Genotoxicity of the food additive E171, titanium dioxide, in the plants *Lens culinaris* L. and *Allium cepa* L. Mutat. Res.- Gen. Tox. En. doi.org/10.1016/j.mrgentox.2020.503142.

Bonilla-Bird, N.J., Paez, A., Hernandez-Viezcas, J.A., Li, C., Peralta-Videa, J.R., Gardea-Torresdey, J.L., 2018. Two-photon microscopy and spectroscopy studies to determine the mechanism of copper oxide nanoparticle uptake by sweetpotato roots during postharvest treatment. Environ. Sci. Technol. 52, 9954–9963.

Boots, B., Russell, C.W., Green, D.S., 2019. Effects of microplastics in soil ecosystems: above and below ground. Environ. Sci. Technol. 53, 11496-11506.

Bosker, T., Bouwman, L.J., Brun, N.R., Behrens, P., Vijve, M.G., 2019. Microplastics accumulate on pores in seed capsule and delay germination and root growth of the terrestrial vascular plant *Lepidium sativum*. Chemosphere 226, 774-781.

Chae, Y., An, Y.J., 2018. Current research trends on plastic pollution and ecological impacts on the soil ecosystem: A review. Environ. Pollut. 240, 387-395.

de Sá, L.C., Oliveira, M., Ribeiro, F., Rocha, T.L., Futter, M.N., 2018. Studies of the effects of microplastics on aquatic organisms: What do we know and where should we focus our efforts in the future? Sci. Tot. Environ. 645, 1029-1039.

de Souza Machado, A.A., Kloas, W., Zarfl, C., Hempel, S., Rillig, M.C., 2018. Microplastics as an emerging threat to terrestrial ecosystems. Glob. Change Biol. 24, 1405–1416.

Deng, Y., Petersen, E.J., Challis, K.E., Rabb, S.A., Holbrook, R.D., Ranville, J.F., Nelson, B.C., Xing, B., 2017. Multiple method analysis of TiO_2 nanoparticle uptake in rice (*Oryza sativa* L.) plants. Environ. Sci. Technol. 51, 10615−10623.

Duis, K., Coors, A., 2016. Microplastics in the aquatic and terrestrial environment: sources (with a specific focus on personal care products), fate and effects. Environ. Sci. Eur. 28, 2.

Geisler-Lee, J., Wang, Q., Yao, Y., Zhang, W., Geisler, M., Li, K., Huang, Y., Chen, Y., Kolmakov, A., Ma, X., 2013. Phytotoxicity, accumulation and transport of silver nanoparticles by *Arabidopsis thaliana*. Nanotoxicology 7, 323–337.

Geyer, R., Jambeck, J.R., Law, K.L., 2017. Production, use, and fate of all plastics ever made. Sci. Adv. 3, e1700782.

Giorgetti, L., Ruffini Castiglione, M., 2016. Oil palm in vitro regeneration: microdensitometric analysis during reproduction and development. Caryologia 69, 5–11.

Giorgetti, L., Spanò, C., Muccifora, S., Bellani, L., Tassi, E., Bottega, S., Di Gregorio, S., Siracusa, G., Sanità di Toppi, L., Ruffini Castiglione, M., 2019. An integrated approach to highlight biological responses of *Pisum sativum* root to nano-TiO_2 exposure in a biosolid-amended agricultural soil. Sci. Tot. Environ. 650, 2705-2716.

Gopinath, P.M., Saranya, V., Vijayakumar, S., Meera, M.M., Ruprekha, S., Kunal, R., Pranay, A., Thomas, J., Mukherjee, A., Chandrasekaran, N., 2019. Assessment on interactive prospectives of nanoplastics with plasma proteins and the toxicological impacts of virgin, coronated and environmentally released-nanoplastics. Scientific Rep. 9, 8860.

Hammer, J., Kraak, M.H., Parsons, J.R., 2012. Plastics in the marine environment: the dark side of a modern gift. Rev. Environ. Contam. Toxicol. 220, 1-44.

Hayes, D., 2019. Micro- and nanoplastics in soil: should we be concerned? Report no. PA-2019-01. Biodegradablemulch.org, USDA.

Hidalgo-Ruz, V., Gutow, L., Thompson, R.C., Thiel, M., 2012. Microplastics in the marine environment: a review of the methods used for identification and quantification. Environ. Sci. Technol. 46, 3060–3075.

Huerta Lwanga, E., Gertsen, H., Gooren, H., Peters, P., Salánki, T., van der Ploeg, M., Besseling, E., Koelmans, A.A., Geissen, V., 2017. Incorporation of microplastics from litter into burrows of *Lumbricus terrestris*. Environ Pollut. 220, 523–531.

ISO 11269- I., 1993. Soil quality- determination of the effects of pollutants on soil flora- Part I. Method for the measurement of inhibition of root growth.

Jana, S., Choudhuri, M.A., 1982. Glycolate metabolism of three submerged aquatic angiosperms during aging. Aquat. Bot. 12, 345–354.

Jeong, C.B., Kang, H.M., Lee, Y.H., Kim, M.S., Lee, J.S., Seo, J.S., Wang, M., Lee, J.S., 2018. Nanoplastic ingestion enhances toxicity of persistent organic pollutants (POPs) in the monogonont rotifer *Brachionus koreanus* via multixenobiotic resistence (MXR) disruption. Environ. Sci. Technol. 52, 11411-11418.

Jiang, X., Chen, H., Liao, Y., Ye, Z., Li, M., Klobučar, G., 2019. Ecotoxicity and genotoxicity of polystyrene microplastics on higher plant *Vicia faba*. Environ. Pollut. 250, 831-838.

Kalčíková, G., ŽgajnarGotvajn, A., Kladnik, A., Jemec, A., 2017. Impact of polyethylene microbeads on the floating freshwater plant duckweed *Lemna minor*. Environ. Pollut. 230, 1108-1115.

Karnovsky, M.J., 1965. A formaldehyde-glutaraldehyde fixative of high osmolality for use in electron microscopy. J. Cell Biol. 27, 137–138.

Kovácik, J., Babula, P., Hedbavny, J., Švec, P., 2014. Manganese-induced oxidative stress in two ontogenetic stages of chamomile and amelioration by nitric oxide. Plant Sci. 215–216, 1–10.

Lian, J., Wu, J., Xiong, H., Zeb,A., Yang, T., Su, X., Su, L., Liu, W., 2020. Impact of polystyrene nanoplastics (PSNPs) on seed germination and seedling growth of wheat (*Triticum aestivum* L.). J. Hazard. Mater. 385, 121620.Mattsson, K., Hansson, L.A., Cedervall, T., 2015. Nano-plastics in the aquatic environment. Environ. Sci. Proc. Imp. 17, 1712–1721.

Ng, E.L., Lwanga, E.H., Eldridge, S.M., Johnston, P., Hu, H.W., Geissen, V., Chen, D., 2018. An overview of microplastic and nanoplastic pollution in agroecosystems. Sci. Total Environ. 627, 1377-1388.

Nolte, T.M., Hartmann, N.B., Kleijn, J.M., Garnæs, J., van de Meent, D., Hendriks, A.J., Baun, A., 2017. The toxicity of plastic nanoparticles to green algae as influenced by surface modification, medium hardness and cellular adsorption. Aquat. Toxicol. 183, 11-20.

Pakrashi S., Jain N., Dalai S., Jayakumar J., Chandrasekaran, P.T., Raichur A.M., Chandrasekaran N., Mukherjee, A., 2014. *In vivo* genotoxicity assessment of titanium dioxide nanoparticles by *Allium cepa* root tip assay at high exposure concentrations. PLoS One 9, e87789.

Pedrosa Gomes, M., Souza Garcia, Q., 2013. Reactive oxygen species and seed germination. Biologia 68, 351-357.

Plastics Europe. Plastics-the facts, 2018. An analysis of European plastics production, demand and waste data Brussels: PlasticsEurope.

Prata, J.C., da Costa, J.P., Lopes, I., Duarte, A.C., Rocha-Santos, T., 2019. Effects of microplastics on microalgae populations: a critical review. Sci. Tot. Environ. 665, 400-405.

Qi, Y., Yang, X., Pelaez, A.M., Huerta Lwanga, E., Beriot, N., Gertsen, H., Garbeva, P., Geissen, V., 2018. Macro- and micro- plastics in soil-plant system: effects of plastic mulch film residues on wheat (*Triticum aestivum*) growth. Sci. Tot. Environ. 645, 1048-1056.

Rilling, M.C., Lehmann, A., Abel de Souza Machado, A., Yang, G., 2019. Microplastic effects on plants. New Phytol. 223, 1066-1070.

Rochman, C.M., Hoh, E., Hentschel, B.T., Kaye, S., 2013. Long-term field measurement of sorption of organic contaminants to five types of plastic pellets: implications for plastic marine debris. Environ. Sci. Technol. 47, 1646−1654.

Ruffini Castiglione, M., Giorgetti, L., Bellani, L., Muccifora, S., Bottega, S., Spanò, C., 2016. Root responses to different types of TiO_2 nanoparticles and bulk counterpart in plant model system *Vicia faba* L. Environ. Exp. Bot. 130, 11–21.

Shukla, R.K., Kumar, A., Pandey, A.K., Singh, S.S., Dhawan, A., 2011. Titanium dioxide nanoparticles induce oxidative stress-mediated apoptosis in human keratinocyte cells. J. Biomed. Nanotechnol. 7, 100-101.

Sjollema, S.B., Redondo-Hasselerharm, P., Leslie, H.A., Kraak, M.H.S., Vethaak, A.D., 2016. Do plastic particles affect microalgal photosynthesis and growth? Aquat. Toxicol. 170, 259-261.

Spanò, C., Bottega, S., Ruffini Castiglione, M., Pedranzani, H.E., 2017. Antioxidant response to cold stress in two oil plants of the genus *Jatropha*. Plant Soil Environ. 63, 271–276.

Sun, X., Chen, B., Li, Q., Liu, N., Xia, B., Zhu, L., Qu, K., 2018. Toxicities of polystyrene nano- and microplastics toward marine bacterium *Halomonas alkaliphila*. Sci. Tot. Environ. 642, 1378-1385.

van Weert, S., Redondo-Hasselerharm, P.E., Diepens, N.J., Koelmans, A.A., 2019. Effects of nanoplastics and microplastics on growth of sediment-rooted macrophytes. Sci. Tot. Environ. 654, 1040-1047.

Wang, Y.S., Ding, M.D., Gu, X.G., Wang, J.L., Pang, Y.L., Gao, L.P., Xsia, T., 2013. Analysis of interfering substances in the measurement of malonildialdehyde content in plant leaves. Am. J. Biochem. Biotechnol. 9, 235–242.

Zhu, D., Chen, Q.L., An, X.L., Yang, X.R., Christie, P., Ke, X., Wu, L.H., Zhu, Y.G., 2018. Exposure of soil collembolans to microplastics perturbs their gut microbiota and alters their isotopic composition Soil Biol. Biochem. 116, 302-310.

Figure legends

Figure 1. Size characterization of nano PS: (a) TEM observation; size distribution of particles grouped in frequency classes for minor (b) and major (c) axis, after ImageJ program elaboration of TEM images.

Figure 2. Mean values of root length in *A. cepa* after 72h of seed imbibition in water (control) and in the presence of 0.01, 0.1, 1 g L^{-1} nano PS. Bars represent standard deviation. Different letters indicated significant differences by *post hoc* Tukey text ($p \leq 0.05$).

Figure 3. Results of cytological analysis of *A. cepa* root meristems after 72h of seed imbibition in water (control) and in the presence of 0.01, 0.1, 1 g L^{-1} nano PS. (a) Mean values of Mitotic index; (b) % of total cytological abnormalities (abnormal metaphases + abnormal ana/telophases); (c) micronuclei frequency (‰). Bars represent standard deviation. Different letters indicated significant differences by *post hoc* Tukey text ($p \leq 0.05$).

Figure 4. Cytological anomalies in *A. cepa* root meristems analysed after 72h of seed imbibition in water (control) and in the presence of 0.01, 0.1, 1 g L^{-1} nano PS; (a, b, c) abnormal c metaphase (1 g L^{-1}); (d, e) sticky metaphases (0.01 and 0.1 g L^{-1}); (f, g) abnormal anaphase with lagging chromosomes and bridges (arrows, 0.1 and 1 g L^{-1}, respectively); (h, i, j) sticky anaphases (h, 0.01 g L^{-1}; i, j, 1 g L^{-1}); (k, l) lagging chromosomes at anaphase (1 g L^{-1}); (m, n) lagging chromosome and micronuclei (arrows 0.1 and 1 g L^{-1} nano PS, respectively).

Figure 5. Cross hand sections of *A. cepa* roots of seedlings after 72 h of seed imbibition in water (control), and in the presence of nano PS. The plate comprehends representative images of: (a) root section of control (toluidine blue staining); (b) central cylinder, (c, d) cortical cylinder, (d) root epidermis in the presence of 1 g L^{-1} nano PS (red spots represent nano PS aggregates, arrows). *In situ* detection of H_2O_2 by Amplex UltraRed Reagent: (e) control; (f, g, h) 0.01, 0.1 and 1 g L^{-1} nano

PS, respectively; *in situ* detection of TBARS by BODIPY reagent: (i) control; (j, k, l) 0.01, 0.1 and 1 g L^{-1} nano PS, respectively.

Figure 6. TEM images of cell portion of *A. cepa* L. (a) control root; (b) 1 g L^{-1} nano PS treated root; (c, d) 0.1 g L^{-1} nano PS treated root; (e, f) 1 g L^{-1} nano PS treated root. The arrows indicate nano PS, the arrow heads indicate electron dense bodies. CR, chromatin; M, mitochondria; N, nucleus; V, vacuole.

Table 1. Germination percentage, hydrogen peroxide (H_2O_2) and thiobarbituric acid reactive substances (TBARS) contents in roots from seeds of *Allium cepa* treated for 72 h with water (C), 0.01, 0.1 and 1.0 g L^{-1} polystyrene nanoparticles.

Parameters	C	0.01 g L^{-1}	0.1 g L^{-1}	1.0 g L^{-1}
Germination %	100.00±0.00a	98.75±2.50a	97.5±2.88a	96.25±2.50a
H_2O_2 (mmol g^{-1} FW)	0.41±0.05b	0.30±0.07b	0.55±0.04b	1.03±0.31a
TBARS (nmol g^{-1} FW)	25.35±0.94b	22.04±0.668c	26.38±1.10b	30.12±1.99a

Values are means of at least four replicates ± SD. Different letters denote significant differences at $p < 0.05$

Table 2 Cytological analysis of *A. cepa* root meristems in control and after 72h treatments with 0.01, 0.1, 1, g/L polystyrene nanoparticles. Normal and abnormal (Abn) mitotic phases (prophases, metaphases and ana/telophases) were expressed as mean values ± standard deviation on 100 mitoses analyzed.

	C	0.01 g L^{-1}	0.1 g L^{-1}	1.0 g L^{-1}
%Prophases	39.6±1.9a	44.3±8.3a	40.8±6.9a	32.7±5.3a
%Metaphases	16.5±4a	10.06±5.8a	9.07±4.3a	9.21±4.1 a
%Abn Metaphases	8.6±4.1a	18.49±2.9b	17.5±3.9b	14.65±3.7ab
%Ana/telophases	27.78±2.4a	20.76±5.5a	17.5±4.8a	26.7±12a
%Abn Ana/telophases	7.5±1.9a	12.7±3.5ab	15.1±4.8ab	16.7±5.5b

Values are means of at least four replicates ± SD. Different letters denote significant differences at $p < 0.05$

Figure 1

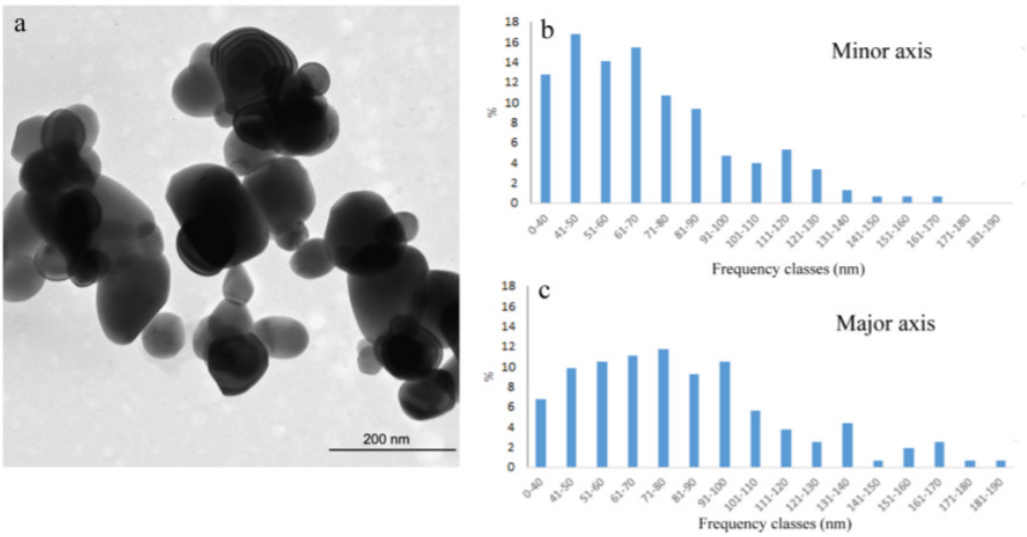

Figure 2

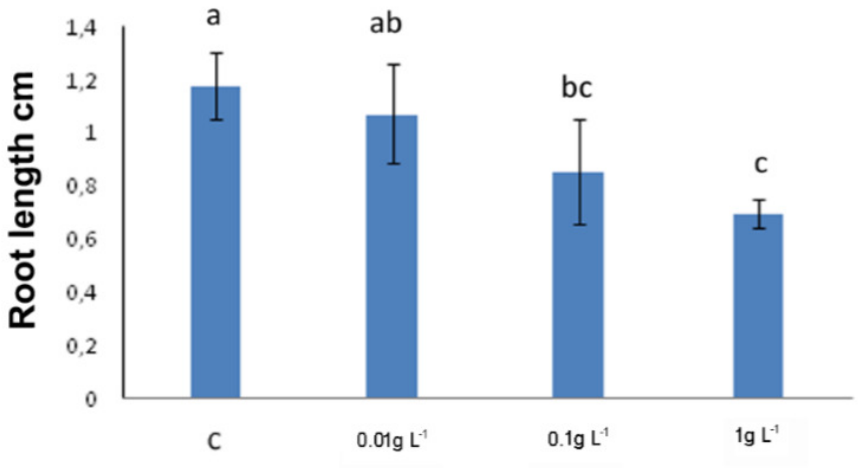

Figure 3

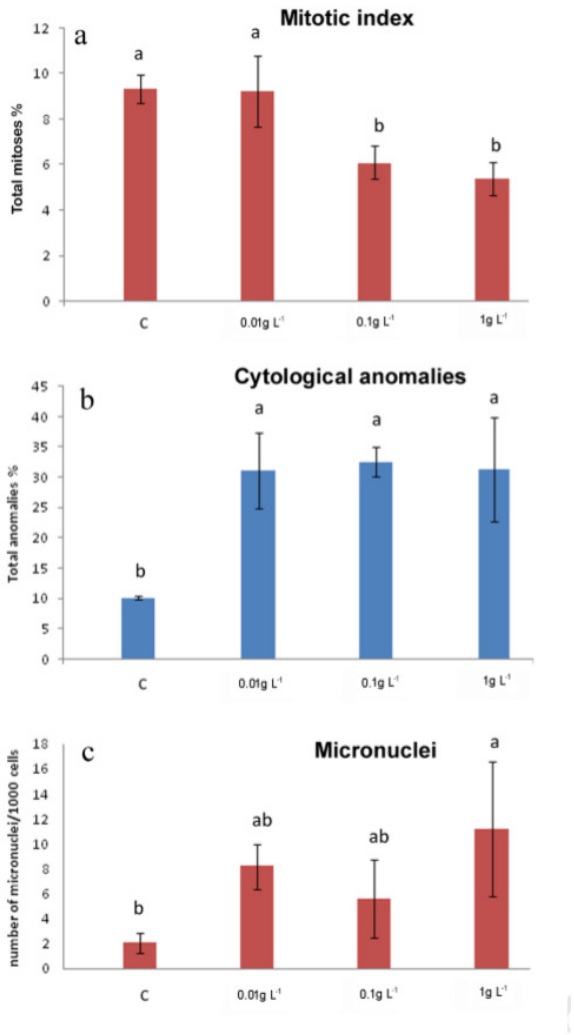

Figure 4

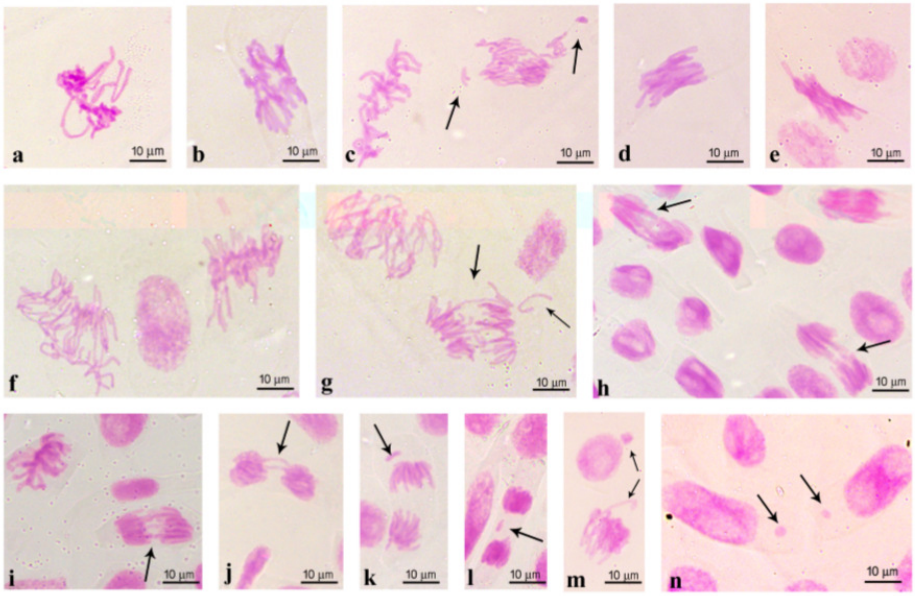

Figure 5

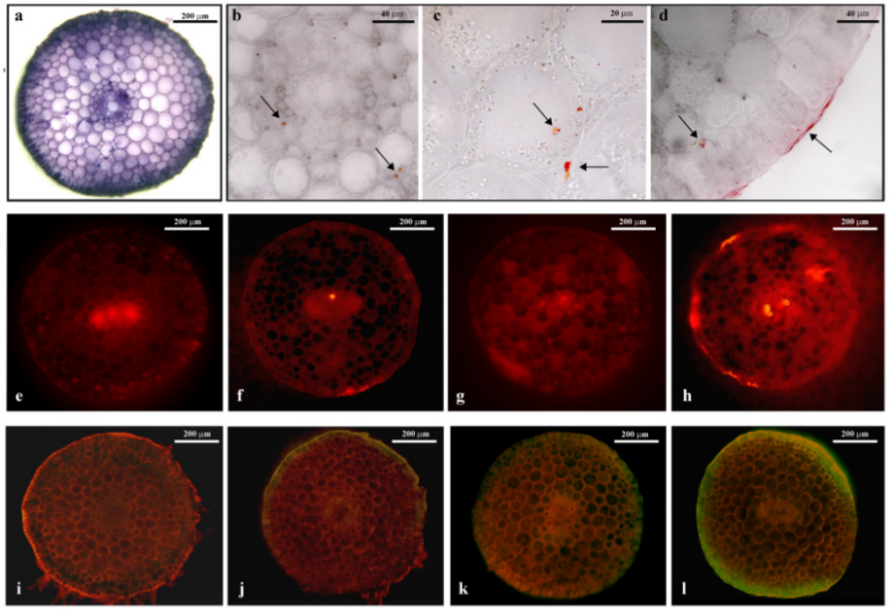

Figure 6